THE JOURNAL OF PHYSICAL CHEMISTRY B

Article

pubs.acs.org/JPCB

Radical Coupling Reactions in Lignin Synthesis: A Density Functional Theory Study

Amandeep K. Sangha,[†] Jerry M. Parks,[†,§,∥] Robert F. Standaert,[‡,∥,⊥] Angela Ziebell,[§,#] Mark Davis,[§,#] and Jeremy C. Smith*[,†,‡,§,∥]

[†]UT/ORNL Center for Molecular Biophysics, Oak Ridge National Laboratory, Oak Ridge, Tennessee 37831-6309, United States

[‡]Department of Biochemistry and Cellular and Molecular Biology, University of Tennessee, Knoxville, Tennessee 37996, United States

[§]Bioenergy Science Center, Oak Ridge National Laboratory, Oak Ridge, Tennessee 37831, United States

[∥]Biosciences Division, Oak Ridge National Laboratory, Oak Ridge, Tennessee 37831, United States

[⊥]Biology and Soft Matter Division, Oak Ridge National Laboratory, Oak Ridge, Tennessee 37831, United States

[#]National Bioenergy Center, National Renewable Energy Laboratory, Golden, Colorado 80401, United States

Supporting Information

ABSTRACT: Lignin is a complex, heterogeneous polymer in plant cell walls that provides mechanical strength to the plant stem and confers resistance to degrading microbes, enzymes, and chemicals. Lignin synthesis initiates through oxidative radical−radical coupling of monolignols, the most common of which are *p*-coumaryl, coniferyl, and sinapyl alcohols. Here, we use density functional theory to characterize radical−radical coupling reactions involved in monolignol dimerization. We compute reaction enthalpies for the initial self- and cross-coupling reactions of these monolignol radicals to form dimeric intermediates via six major linkages observed in natural lignin. The 8-O-4, 8-8, and 8-5 coupling are computed to be the most favorable, whereas the 5-O-4, 5-5, and 8-1 linkages are less favorable. Overall, *p*-coumaryl self- and cross-coupling reactions are calculated to be the most favorable. For cross-coupling reactions, in which each radical can couple via either of the two sites involved in dimer formation, the more reactive of the two radicals is found to undergo coupling at its site with the highest spin density.

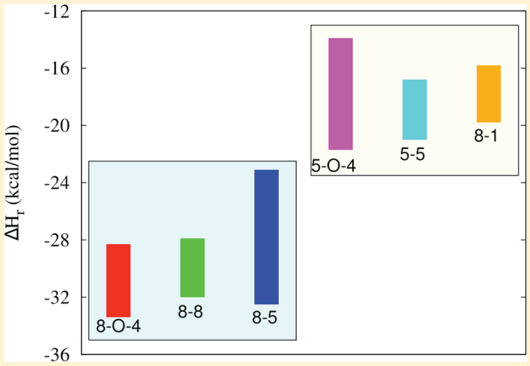

1. INTRODUCTION

Lignin, which constitutes 15−30% of plant biomass,[1] has been of interest in the wood, paper, and pulp industries for many decades[2−5] and more recently has gained further attention due to the importance of cellulosic biomass in biofuel production.[6−9] Along with other factors such as cellulose crystallinity,[10] lignin is a primary contributor to the recalcitrance of biomass to hydrolysis, binding covalently to hemicellulose and forming cross-links with cellulose,[11,12] hindering access of deconstructing reagents.

The structure of lignin is complex and heterogeneous. It is composed mainly of three cinnamyl alcohol constituents: *p*-coumaryl, coniferyl, and sinapyl alcohol (Figure 1). These monolignols are incorporated into polymeric lignin as *p*-hydroxyphenyl (H), guaiacyl (G), and syringyl (S) units, respectively, and are covalently linked through various C−O and C−C bonds. Monolignols are synthesized in the cytoplasm and transported across the cell membrane to the lignification zone in the cell wall,[13,14] where they undergo enzymatic oxidation (dehydrogenation). Laccase and peroxidase enzymes are involved in this oxidation, but the exact mechanism of radical formation is unclear.[5,15,16] Lignin is synthesized by

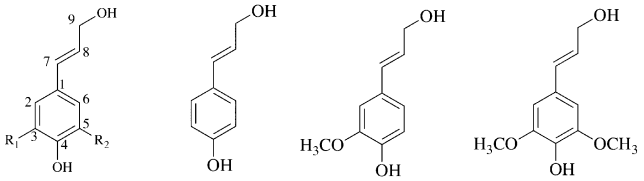

Figure 1. Atom numbering and chemical structures of the three most common monolignols: *p*-coumaryl, coniferyl, and sinapyl alcohols.

oxidative coupling of the monomers to the growing polymer chain.[3,11,17−19]

It is difficult to characterize the structure of lignin experimentally because of its structural heterogeneity and insolubility. Experimental techniques such as nuclear magnetic resonance (NMR), infrared (IR), and Raman spectroscopies, analytical pyrolysis, and thermal analysis have revealed useful

Received: December 19, 2011
Revised: April 3, 2012
Published: April 4, 2012

   dx.doi.org/10.1021/jp2122449 | *J. Phys. Chem. B* 2012, 116, 4760−4768

Scheme 1. Initial Step of Radical−Radical Coupling of Monolignol Radicals during Lignin Synthesis[a]

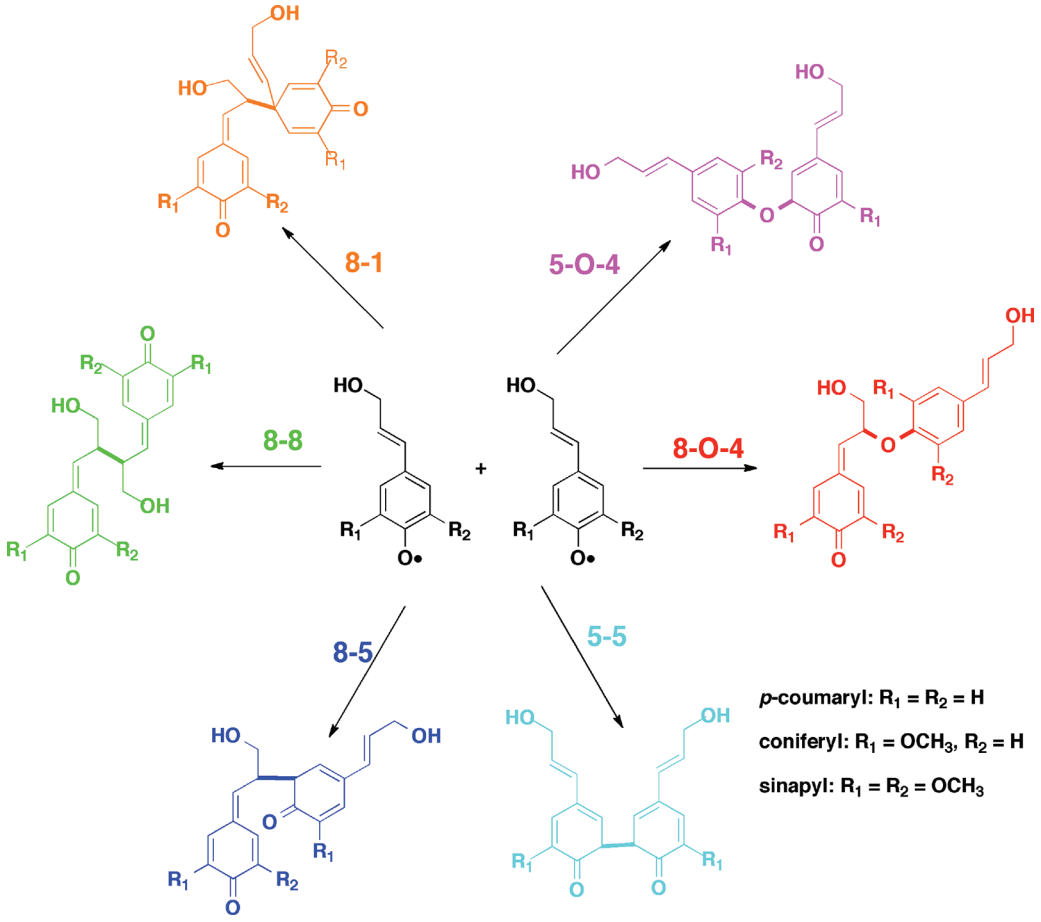

[a]Two radicals can undergo coupling at various sites to form different interunit C−O and C−C bonds. Stereochemistry is omitted for simplicity. The R_2 substituent is omitted in the 5-5, 5-O-4, and 8-5 linkages because coupling of sinapyl radical via C5 is not considered here.

but limited information. For example, 2D-NMR can be used to determine the relative abundance of different lignin units and interunit linkages.[20] However, the lignin must be isolated from the whole biomass and dissolved, or the whole biomass must be dissolved, which can be technically challenging and time-consuming. Analytical pyrolysis can be used to determine lignin content and the S/G ratio,[21] and thermal analysis can be used to measure the stabilities and probabilities of different linkages.[8,9,22−26]

Only a small number of classical dynamics or quantum chemical studies have hitherto been performed to study the formation of dilignols and their structures.[27−35] Structures of guaiacyl, syringyl, and *p*-hydroxyphenyl 8-O-4 homodimers have also been characterized in vacuo and in explicit solvent using classical molecular dynamics simulations.[31−34] Quantum chemical studies have focused mainly on the coniferyl monomer (guaiacyl unit) and the aryl-ether (8-O-4) linkage, because 8-O-4 is the predominant interunit linkage observed in natural lignin and guaiacyl units are present in all types of lignin including softwood (which consists mainly of G), hardwood (S and G), and grasses (H, G and S). In a recent study,[36] several mechanisms for the formation of 7-O-4 linked coniferyl alcohol dimers were investigated using density functional theory (DFT). Reaction free energies were computed for dimerization reactions, and fukui functions were used to determine the most reactive sites on the radical intermediates. Also, DFT studies of the bond dissociation enthalpies of various C−C and C−O linkages in native and modified lignin dimers have provided insight into the thermal degradation of lignin.[8,9] These studies have focused on substituent effects on bond dissociation[8] and identified targets for catalytic cleavage during thermal decomposition.[9]

Spin densities have been used previously to understand the effect of methoxylation of the phenolic ring on the ease of monolignol radical formation and the reactivity of radicals thus formed.[37] The regioselectivity of radical−radical coupling is at least partially determined by the distribution of unpaired electron spin in the radicals, and computed spin densities are presumed to correlate with experimentally observed linkages. That is, high electron spin density at a particular site indicates high reactivity at that site.

The relative thermodynamic stabilities of lignin dimers formed via various interunit linkages are likely to influence the linkage distributions in lignin.[28,29] Enthalpy changes have been examined for self-coupling reactions of coniferyl radicals at the B3LYP/6-31+G(d,p) level of theory with a polarized continuum representation of the surrounding medium.[28] Although 8-O-4 is the most common linkage in natural lignin, that study found that the 8−8 linked dimer is enthalpically the most stable of the 8-O-4, 8-8, 8-5, 8-1, 5-5, and 5-O-4 coniferyl dimers.[29]

To further our understanding of factors that determine linkage distributions in lignin, a complete study of the radical−radical coupling reactions of all three major monolignol radicals

dx.doi.org/10.1021/jp2122449 | J. Phys. Chem. B 2012, 116, 4760−4768

via various interunit linkages is desirable, and this is provided here. We focus on coupling reactions of monolignol radicals to form dimeric intermediates, and Scheme 1 shows representative coupling products for each type of linkage considered. We consider a total of 39 coupling reactions encompassing six different linkages and identify the most stable stereoisomeric products. Low-energy conformers are identified for each linkage, which we expect to be close to the global minima. Electron spin densities of the monolignol radicals are examined, and gas-phase and solvated reaction enthalpies of the radical coupling reactions are calculated and compared.

2. METHODS

To identify low-energy conformers for each reaction product, a multistep procedure was used. Arbitrary starting conformations were generated for all possible stereoisomers of the alcohols and dimers. From these initial geometries, Monte Carlo conformational searches were performed using the MM3 force field,[38] as implemented in the Tinker suite of programs.[39] In each case, at least 500−14000 conformations were generated and minimized. The ten lowest energy conformers for each compound were then optimized at the B3LYP/6-31+G(d,p) level of theory[40,41] using the program NWChem.[42] For the monolignol radicals, the O4 hydrogen was removed from the corresponding alcohol conformers, and the structures were optimized using B3LYP. The single lowest energy conformer for each species was then reoptimized using the ωB97X-D density functional[43] and the 6-31+G(d,p) basis set with the program Gaussian09.[44] ωB97X-D, a range-separated double-hybrid functional, has been shown to describe reaction energies accurately.[45] We also tested several larger basis sets and found that 6-31+G(d,p) performed well (see Supporting Information). Recently, benchmark calculations on model 8-O-4-linked dimers showed that relative trends in bond dissociation energy computed using the ωB97X-D density functional are in agreement with CBS-QB3 energies, although absolute energies were underestimated by ∼3−4 kcal/mol.[9] Open- and closed-shell formalisms were applied for the radicals and dimeric intermediates, respectively. Vibrational frequencies were computed to confirm that all optimized structures were true minima. Electron spin densities based on Natural Bond Orbital[46] (NBO) analyses were used to quantify the degree of unpaired spin at various sites in radical species. All of the above calculations were performed in the gas phase.

Bond dissociation energies (BDEs), radical stabilization energies (RSEs), and reaction enthalpies (ΔH_r) including zero-point vibrational energy (ZPVE) corrections were computed for the six interunit linkages observed in lignin: 8-O-4, 8-8, 8-5, 8-1, 5-5, and 5-O-4. Reaction enthalpies, reaction free energies (neglecting the conformational entropy contributions) for all coupling reactions, and optimized geometries of the lowest energy conformers identified for all alcohols, radicals, and dimers are provided as Supporting Information.

3. RESULTS

We first examined the structures of the monolignols and their corresponding radicals and calculated their relative stabilities. Electron spin densities for the monolignol radicals were compared and the dimer geometries described. Gas-phase and continuum-solvated reaction enthalpies for the radical coupling reactions were calculated and compared, and finally, the thermodynamics of dilignol formation from the dimeric intermediates by hydration and rearomatization/tautomerization were characterized.

3.1. Geometries of the Monolignols and the Radicals.

The optimized structures of the three phenolic radicals are shown in Figure 2. All substituent groups, i.e., hydroxy, methoxy, and double bond, are coplanar with the aromatic ring. The allylic alcohol group in the three monolignols adopts the *syn* orientation relative to the phenolic OH group. Consistent with previous work,[47] the allylic alcohol moiety adopts the (ac, sc) conformation, with the C−O bond ∼120° out of the plane of the double bond and the hydrogen oriented back toward the double bond. For coniferyl alcohol, the phenolic hydrogen is hydrogen-bonded to the adjacent methoxy group. The lowest energy conformers of the *p*-coumaryl and sinapyl radicals were found to share the same overall conformations with their respective monolignols, except that the phenolic hydrogen has been removed (Figure S1 of Supporting Information). Further consideration was given to the rotation of the 3/5 *O*-methyl groups in coniferyl and sinapyl radicals. Previous studies[48,49] have found different conformational preferences in the monolignols and their derived radicals. In coniferyl alcohol, the preferred conformation features a hydrogen bond from the phenolic oxygen to O3, with the methyl group rotated toward C2. In coniferyl radical, however, the preferred conformer has the methyl group rotated 180° toward the phenolic oxygen. Accordingly, we investigated the different rotameric possibilities for the methyl group in coniferyl and sinapyl radicals. Consistent with previous work, we also found that the preferred conformation of coniferyl radical has its O3-methyl oriented toward the phenolic oxygen at C4 rather than toward C2. At the B3LYP/6-31+G(d,p) level of theory, the energy difference was 1.1 kcal/mol. However, at the ωB97X-D/6-31+G(d,p) level of theory, the difference was only 0.05 kcal/mol. For sinapyl radical, we found that the B3LYP/6-31+G(d,p) level of theory predicts the most stable conformation to have one methyl rotated toward the phenolic oxygen and the other away.[48] However, at the ωB97X-D/6-31+G(d,p) level, there is a strong preference for the conformation with both methyl groups rotated away from the phenolic oxygen. The penalty for having one or both methyl groups rotated toward the phenolic oxygen is 0.5 or 1.7 kcal/mol, respectively. These findings suggest that dispersive effects play a significant role in the conformational preferences of coniferyl and sinapyl radicals.

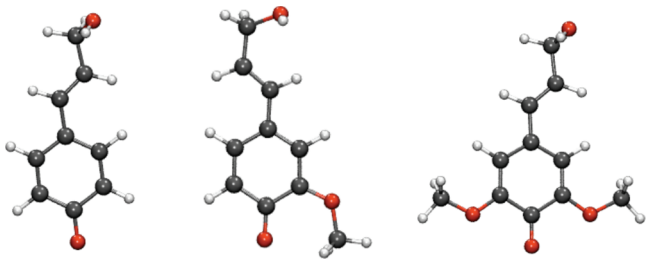

Figure 2. Lowest energy structures identified for *p*-coumaryl, coniferyl, and sinapyl alcohol radicals (left to right). The syn orientation of the vinyl group determined previously for the monolignols[47] is preserved in *p*-coumaryl and sinapyl radicals.

3.2.1. Monolignol Radical Formation: Bond Dissociation and Radical Stabilization Energies. Prior to polymerizing, monolignols must undergo oxidation by abstraction of their phenolic hydrogens to form phenolic radicals. The energetic

dx.doi.org/10.1021/jp2122449 | J. Phys. Chem. B 2012, 116, 4760−4768

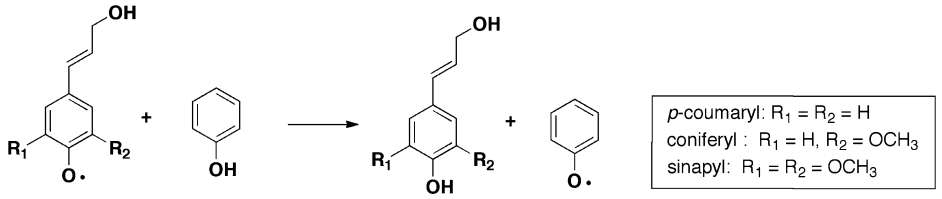

Figure 3. The enthalpy change for the reaction shown above gives the radical stabilization energy (RSE) for the monolignol radicals. RSEs for *p*-coumaryl, coniferyl, and sinapyl radicals relative to phenoxyl radical are shown in Table 1.

cost of this oxidation may in principle affect the linkage distribution in polymeric lignin, particularly in nonenzymatic syntheses. Although hydrogen abstraction is an enzymatically mediated process in plants, in which differential binding affinities and other effects may affect oxidation rates among the monolignols, the BDEs of the resulting radicals are directly related to their intrinsic reactivities in coupling reactions.

Here, we compare and quantify the energetics of monolignol oxidation by computing homolytic BDEs and RSEs[50,51] of the phenolic O−H bond. RSEs are computed as the difference between the BDE of a given species and the BDE of a reference molecule, in this case phenoxyl radical. In relation to BDEs, RSEs are expected to be more reliable and comparable to other data because systematic errors arising from a particular theoretical method cancel out. Positive RSEs correspond to increased radical stability relative to the reference molecule. For all three radicals, RSEs were calculated by considering the enthalpy change for the isodesmic reaction shown in Figure 3.

Table 1 shows the BDEs and RSEs for the phenolic OH bond in the three monolignols. The BDE is lowest for sinapyl

Table 1. Bond Dissociation Energies and Radical Stabilization Energies[a] (kcal/mol) for the Phenolic O−H Bond Computed at the ωB97X-D/6-31+G(d,p) Level of Theory

monolignol	BDE (rel[b])	RSE[a]
p-coumaryl	81.1 (2.9)	2.9
coniferyl	81.4 (3.2)	2.6
sinapyl	78.2 (0.0)	6.0

[a]Computed using phenol as the reference molecule. [b]Relative to sinapyl alcohol.

alcohol (78.2 kcal/mol) indicating that, of the three radicals, sinapyl is the easiest to form. Somewhat unexpectedly, coniferyl radical was found to have the highest BDE (81.4 kcal/mol). On the basis of the RSE calculations, it is possible to quantify the effects of the methoxy and allylic alcohol substituents on radical stability. The allylic alcohol group at the para position relative to the phenolic oxygen in *p*-coumaryl radical provides 2.9 kcal/mol of stabilization relative to phenoxyl radical, and the methoxy group in coniferyl radical is slightly destabilizing by 0.3 kcal/mol relative to the *p*-coumaryl radical. The coniferyl radical is more stable than the phenoxy radical by 2.6 kcal/mol. Sinapyl radical was computed to have the highest RSE, indicating that it is the most stable of the three radicals. The net effect of the two methoxy groups and the allylic alcohol in sinapyl radical provides an overall stabilization energy of 6.0 kcal/mol relative to phenoxyl radical.

3.2.2. Electron Spin Densities for Monolignol Radicals. Resonance theory predicts the presence of radical character at specific sites, but spin density calculations quantify the amount of unpaired spin at these positions and thus provide additional insight into the origins of regioselectivity in radical coupling reactions. Electron spin density is defined as the difference between the total electron spin densities of electrons with α spin and β spin. All other things being equal, higher spin density at a given site suggests that the site is likely to be more reactive. Semiempirical calculations using the AM1 method[52] suggested an electron donating effect of the methoxy groups on the distribution of electron spin density in monolignol radicals, such that the presence of a methoxy group on the aromatic ring increases the spin density on the hydroxyl oxygen in sinapyl and coniferyl radicals.[53]

Spin densities have been found to be significantly less sensitive to the choice of the particular population analysis scheme than are atomic partial charges.[54] NBO-based spin densities obtained using the ωB97X-D functional for the three monolignol radicals are shown in Figure 4. C1 has the highest

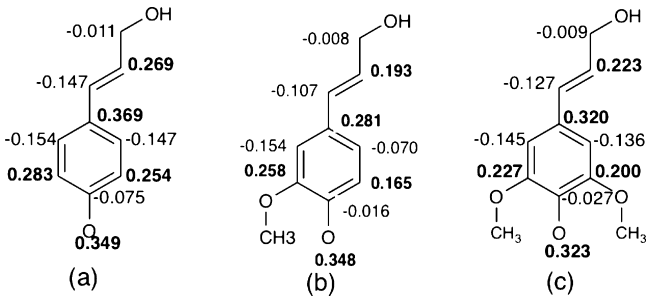

Figure 4. ωB97X-D spin densities computed using NBO analysis for (a) *p*-coumaryl, (b) coniferyl, and (c) sinapyl radicals.

spin density in *p*-coumaryl radical, followed by O4, C3, C8, and C5. In coniferyl and sinapyl radicals, O4 has the highest spin density followed by C1, C3, C8, and C5. Lower RSE, coupled with higher spin density at equivalent sites, suggests that *p*-coumaryl radical may be more reactive than coniferyl and sinapyl radical. In the present calculations, it was found that spin density on O4 relative to C1, C3, C5, or C8 increases in the order *p*-coumaryl < sinapyl < coniferyl radical (Figure 4), indicating that O4 becomes more reactive as successive methoxy substituents are added at C3 and C5.

Despite the high spin density at C1, coupling to this position occurs at low frequency in natural lignin.[4] Moreover, linkages to C1 are believed to form only at the growing end of lignin chains after coupling to C8 and saturation of the C7−C8 double bond have already occurred.[55,56] Thus, reaction at C1 occurs under a narrow set of circumstances and is not a generally favored pathway for free monolignol radicals. Coupling at other substituted positions on the ring (C3 in coniferyl, C3 and C5 in sinapyl) occurs to an inconsequential extent if it occurs at all. A likely explanation is that non-hydrogen substitutents at the coupling site create steric hindrance, making the couplings less exothermic, and block subsequent rearomatization. Overall, O4

dx.doi.org/10.1021/jp2122449 | J. Phys. Chem. B 2012, 116, 4760−4768

and C8 emerge as the most likely coupling sites, with the *p*-coumaryl radical predicted to be the most reactive based on spin density. For *p*-coumaryl radical, C3 and C5 sites are equally viable and indistinguishable for coupling reactions.

3.3. Dimer Geometries. Geometries for self- and cross-coupling products were optimized using a multistep procedure in which conformational searches were carried out to identify low-energy conformers (see Methods). Apart from cross-coupling reactions involving 5-5 and 8-8 linkages, any two monolignol radicals can undergo a given coupling reaction in two possible orientations. For example, in the case of the 8-O-4 cross coupling of *p*-coumaryl radical (H) with coniferyl radical (G), either the H^{C8}-G^{O4} or the H^{O4}-G^{C8} quinone methide can be formed (Figure S9 of Supporting Information) and the same is true for the 8-1, 8-5, and 5-O-4 linkages (except for dimers involving sinapyl radical, for which C5 is not a viable coupling site). Hence, when different combinations of sites on the participating radicals can form the same linkage type, all possibilities were considered. Likewise, many couplings can give rise to stereoisomeric products. In these cases, we considered each diastereomer separately. Where enantiomers could form, we considered only one of each pair as enantiomers have identical energies and mirror-image conformational populations.

Substituent effects originating from the presence or absence of methoxy groups on each monomer manifest themselves in various ways in the resulting dimeric intermediates. Aside from contributing steric and inductive effects, methoxy groups can also serve as hydrogen bond acceptors. Dispersion effects may also play a role in determining interunit orientations.

The optimized geometries of the self- and cross-coupled dimeric intermediates are described in detail in the Supporting Information. It was found that, depending on the three-dimensional arrangement of monomer subunits permitted by the specific linkage under consideration, intramolecular hydrogen bonds may be formed by allylic hydroxyl groups or the methoxy groups when present. Also, the structures of 8-8 and 8-5 linked dimeric intermediates obtained using the ωB97X-D functional are more compact than the B3LYP optima (not shown). Although the forms of these two functionals are quite different, it is reasonable to assume that attractive dispersion interactions between the aromatic systems in the monomer subunits may be responsible for the conformational differences, for two reasons. First, B3LYP does not account for dispersion effects, and second, the conformational differences between the B3LYP and ωB97X-D minima for all other dimeric intermediates (except 8-8 and 8-5 linked dimers) were small.

3.4. Gas-Phase Reaction Enthalpies of Radical Coupling Reactions. *3.4.1. Self-Coupling Reactions.* Figure 5 shows the computed ΔH_r values for the self-coupling of the three monolignol radicals via six interunit linkages. These values were calculated for formation of the most stable conformer of the most stable stereoisomer in each case. The reaction enthalpies can be roughly partitioned into two groups. The dimeric intermediates in the first group, consisting of 8-O-4, 8-8, and 8-5, are ~5−20 kcal/mol more stable than those of the second group, 5-O-4, 5-5, and 8-1. For all linkage types, the self-coupling reaction of the *p*-coumaryl radical is enthalpically the most favorable of the three monolignols.

3.4.2. Cross-Coupling Reactions. As was found in the self-coupling reactions, the cross-coupling ΔH_r values for 5-O-4, 5-5, and 8-1 linked dimers are much less favorable (by 15 kcal/mol) than the 8-O-4, 8-8, and 8-5 dimers, with the exception of

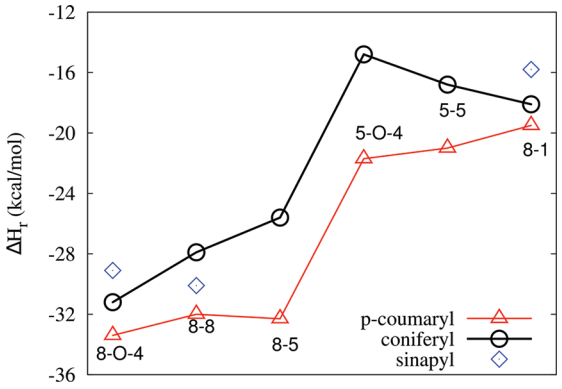

Figure 5. Reaction enthalpies (ΔH_r) for the self-coupling of *p*-coumaryl, coniferyl, and sinapyl radicals via various linkages. Self-coupling of *p*-coumaryl radical is enthalpically the most favorable of all three radicals and linkage types. Linkages involving C3 and C5 of sinapyl radical were not considered here. However, 8-1 linkages have been observed in natural lignin;[4] so these linkages were also included in the calculations.

S^{C8}-X^{C5} reactions, where X = H or G, which are somewhat less favorable in the cross-coupling case (Figures S2 and S3 of Supporting Information). Thus, calculations indicate that the enthalpic trend remains similar for self- and cross-coupling reactions of *p*-coumaryl radical. The reaction enthalpies for 8-8, 8-5 and 5-O-4 cross coupling reactions of coniferyl with *p*-coumaryl radical become more favorable by ~3−7 kcal/mol than those for coniferyl self-coupling reactions (Figure S4 of Supporting Information), indicating that coniferyl radical has a preference for cross coupling rather than self-coupling.

3.5. Solvent Effects. To investigate the effects of solvation on reaction enthalpies and free energies, the lowest energy conformer at the B3LYP/6-31+G(d,p) level of theory for each monomer radical and dimeric intermediate was reoptimized at the ωB97X-D/6-31+G(d,p) level of theory in the presence of a polarized continuum model (IEF-PCM).[57] Dielectric constants of 4.24, 24.85, and 78.35 were used to represent diethyl ether, ethanol, and water, respectively.

The major conclusions from the gas-phase calculations were unchanged by the presence of the three continuum solvents. The three linkages computed to be the most favorable for self-coupling of the *p*-coumaryl radical, i.e., 8-O-4, 8-8, and 8-5, remain more favorable than the other three linkages, 5-O-4, 5-5, and 8-1 (Figure S6 of Supporting Information). However, for all three radicals, the reaction enthalpy for any given radical coupling reaction becomes less negative (by ~0−5 kcal/mol) in going from the gas phase to ether solvent (ε = 4.24) and even less negative (by ~5−6 kcal/mol) for the higher dielectric constants of 24.85 and 78.35 (Figures S6 and S7 of Supporting Information).

For *p*-coumaryl coupling reactions, the 8-8 and 8-1 linkage reaction enthalpies and reaction free energies are affected least by the presence of solvent. At the higher dielectic constants of 24.85 and 78.35, the linkage favorability trend changes to 8-8 > 8-O-4 > 8-5 from the 8-O-4 > 8-8 > 8-5 trend in the gas phase, although the enthalpy differences are quite small and likely insignificant (Figure S6 of Supporting Information). The linkage trend for coupling reactions involving coniferyl and sinapyl radicals is not affected by solvation (Figure S7 of Supporting Information). For coniferyl radical, the reaction enthalpies for 8-8 coupling in continuum solvent with various dielectric contants are lower than gas-phase reaction enthalpies.

dx.doi.org/10.1021/jp2122449 | J. Phys. Chem. B 2012, 116, 4760−4768

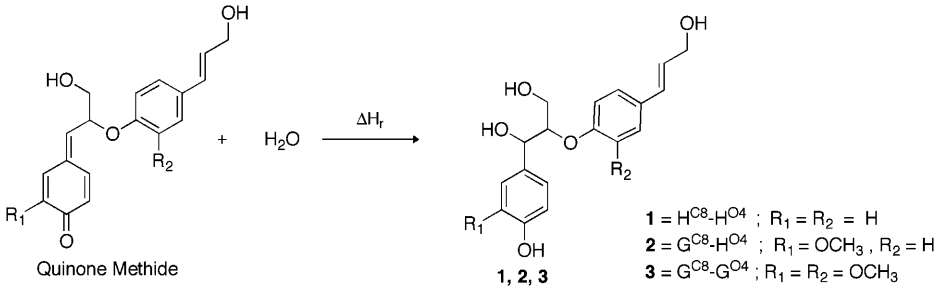

Figure 6. Nucleophilic addition of a water molecule to the quinone methide yields a dilignol.

Consistent with the results from gas-phase calculations, coupling reactions in the continuum solvents involving *p*-coumaryl radical were also found to be enthalpically more favorable than those involving coniferyl or sinapyl radical.

3.6. Thermodynamics of Dilignol Formation from Dimeric Intermediates. The calculations up to this point have characterized the initial product of radical couplings. These compounds are in most cases intermediates in which one or both rings have lost aromaticity and undergo further reaction to give the stable, fully aromatic products customarily regarded as dilignols. Here, we consider the two most general rearomatization pathways, hydration of quinone methides and tautomerization of cyclohexadienones. For each pathway, gas-phase reaction enthalpies were calculated. In some cases, other rearomatization pathways are available, for example, the intramolecular cyclization of the 8-8 coupling products into 3,7-dioxa[3.3.0]octanes (resinols) or of the 5−8 coupling products into 2,3-dihydrobenzofurans (phenylcoumarans). As these products are particular to specific coupling orientations, and can at least conceptually be considered downstream products of hydrated or tautomerized dimers, they are not considered here. Coupling at sites where spin density is ample but rearomatization is not possible, i.e., C1, C3 of coniferyl or sinapyl and C5 of sinapyl, is not generally observed in natural lignin.

3.6.1. Quinone Methide Hydration. Nucleophilic addition of a water molecule to C7 of a quinone methide leads to rearomatization of the ring (Figure 6). The reaction enthalpies for the hydration of H^{C8}-H^{O4}, G^{C8}-H^{O4}, and G^{C8}-G^{O4} quinone methides were calculated to be −25.8, −26.7, and −29.1 kcal/mol, respectively (Table 2). When added to the enthalpies for the first step, i.e., initial radical−radical coupling, the overall reaction enthalpies were found to be around −60 kcal/mol and are thus highly favorable.

Table 2. Reaction Enthalpies for Quinone Methide Formation (ΔH_r I), Hydration of Quinone Methide to (ΔH_r II), and Overall Reaction Enthalpies (Total ΔH_r) for the Dilignol Formation Reaction Shown in Figure 6

dilignol	ΔH_r I (kcal/mol)	ΔH_r II (kcal/mol)	total ΔH_r (kcal/mol)
H^{C8}-H^{O4}	−33.4	−25.8	−59.2
G^{C8}-H^{O4}	−33.2	−26.7	−59.9
G^{C8}-G^{O4}	−30.9	−29.1	−60.0

3.6.2. Rearomatization/Tautomerization. Dimeric intermediates formed via 8-8 and 8-5 linkages can undergo tautomerization to regain ring aromaticity during dilignol formation. To exemplify this process, a model reaction, tautomerization of 2,4-cyclohexadienone to phenol, was considered (Figure 7). The enthalpy change for this reaction, calculated at the ωB97X-D/6-31+G(d,p) level of theory, is −16.7 kcal/mol, indicating that the second step in the formation of 8−8 and 8−5 linked dilignols is also thermodynamically favorable, though to a lesser extent than hydration of an 8-O-4 linked quinone methide.

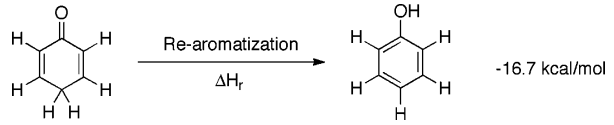

Figure 7. Model rearomatization reaction involved in dilignol formation.

4. DISCUSSION

The present work reports on quantum chemical studies of the enthalpy of coupling for the three most common radicals in lignin synthesis: *p*-coumaryl, coniferyl and sinapyl radical, examining both self- and cross-coupling. Though previous work has examined the reactivity and structures of coniferyl alcohol,[28,29] this work is the first comprehensive study of these important coupling reactions.

Initial coupling reactions in lignin synthesis involve two distinct chemical steps. In the first step, two radicals undergo coupling to form a dimeric intermediate. If a kinetic barrier exists for this first step, it is expected to be quite low. Barriers have been estimated to be on the order of ∼2−5 kcal/mol based on DFT calculations,[28] though also as high as 9.8 kcal/mol based on semiempirical calculations.[58] In the second step, the dimeric intermediate can undergo tautomerization or nucleophilic addition of water to form rearomatized products. The barriers for the second steps have not been determined.

The initial coupling reactions can be divided into two groups (Figure 5): those that involve C8 and are strongly exothermic ($\Delta H_r \lesssim -22$ kcal/mol) and those that do not involve C8 and are weakly exothermic ($\Delta H_r \gtrsim -22$ kcal/mol). Uniformly, coupling via the 8-O-4 linkage is most thermodynamically favorable, as has been observed experimentally.[11] The 8-8 linkage and the 8-5 linkage at unsubstituted sites are also strongly favorable, whereas the 5-O-4 and 5-5 couplings are distinctly less favorable. In many of the dimers formed, and especially those involving coniferyl and sinapyl radicals, an intramolecular hydrogen bond calculated here to be of strength ∼3−4 kcal/mol exists. These hydrogen bonds were found to persist in the presence of continuum solvent, although such a solvent description precludes formation of specific solute−solvent hydrogen bonding. Self-coupling of *p*-coumaryl radical was found to be at least as favorable as cross-coupling for all linkage types. For the coniferyl and sinapyl radicals, cross-coupling with *p*-coumaryl is always more favorable than the self-coupling reaction.

dx.doi.org/10.1021/jp2122449 | J. Phys. Chem. B 2012, 116, 4760−4768

For cross-coupling reactions it is found here that for two monolignol radicals undergoing coupling via a particular linkage there exists a correlation between the spin density of the more reactive radical of the two and the linkage site through which that radical couples. To give a few examples, in the case of the 8-O-4 linkage between the *p*-coumaryl and coniferyl radicals, *p*-coumaryl is more reactive and thus determines which *p*-coumaryl site (C8 or O4) participates in the 8-O-4 linkage: as the spin density on O4 is higher than that of C8, we can expect *p*-coumaryl coupling via O4 to be favored. The other radical, coniferyl in this case, will then couple via C8. Thus, H^{O4}-G^{C8} is predicted to be more favorable than G^{O4}-H^{C8}, although the energy difference in this case is only ∼2 kcal/mol and may not be significant. The analysis also suggests that S^{C8} -H^{O4} is slightly more favorable than H^{C8}-S^{O4}. Similarly, in the case of the 8-5 linkage, *p*-coumaryl, being the most reactive, has a higher spin density at C5 than C8 and thus should react via C5. The same argument holds for the 8-1 and 5-O-4 linkages. The spin densities at C5 and O4 differ only slightly, as do the reaction free energies for coupling via either site. According to the present calculations, coniferyl reacts via C8 to O4 of sinapyl radical during 8-O-4 coupling reaction.

For radical coupling reactions with small barriers, one expects that spin density in the radicals, rather than thermodynamic stability of the products, is the best predictor of regioselectivity. If one considers the productive coupling sites in the lignol radicals, i.e., O4, C8, and unsubtituted C5 positions, the spin density and thermodynamic preferences are correlated. The highest spin density always resides at O4, and C−O4 couplings are the most strongly exothermic. The *p*-coumaryl radical has higher spin density at C5 than at C8, and coupling at C5 is slightly favored where there is a choice (H−H and H−G pairs). Conversely, coniferyl radical has higher spin density at C8 than at C5 as well as a greater enthalpic preference for coupling at C8 where there is a choice (G−G and G−H pairs).

Proper analysis of coupling preferences involves consideration of free energy rather than enthalpy alone. For dimerization reactions in general, one expects a strongly negative entropy change, both at the transition state ($\Delta S^{\ddagger}$) and in the product (ΔS^{0}). We have estimated the free energy changes for the coupling reactions by considering rotational, translational, and vibrational entropy and found that the magnitude of $T\Delta S$ is in the range 13−20 kcal/mol at 25 °C (Table S2 of Supporting Information). A rigorous analysis would also include conformational entropy change, but performing quantum calculations on the entire conformational populations was not feasible. From the molecular mechanics simulations, we estimate that conformational entropy change is relatively minor, e.g., $T\Delta S$ is on the order of 2−3 kcal mol for the G^{O4}-G^{C8}e dimer. While all of the reactions remain favorable when free energy is considered, they are considerably less favorable than one would expect on enthalpic considerations. The 5-O-4 and 5-5 couplings in particular are only weakly favorable (ΔG^{0}_{est} = −1.1 to −8.4 kcal/mol). An interesting possibility suggested by our results is that the initial coupling reactions may be reversible, especially for the less favorable 5-O-4 and 5-5 couplings. To what extent reversibility influences product distribution depends both on the activation parameters for the specific coupling under consideration as well as the rates of downstream reactions, such as hydration and tautomerization.

Modification of the composition of lignin in plants provides an approach for improving sugar release from lignocellulosic biomass during processing.[59−61] As processing is a large percentage of overall biofuel production costs, this point is of both academic and commercial importance. High S/G ratio and high H content in lignin have been related to increased sugar release.[62] Furthermore, lignin rich in H units has been shown to be relatively easily deconstructable.[63]

In lignin with high H content, it has been observed experimentally that the prevalence of 8-O-4 bonds decreases and those of 8−5 and 8−8 increase.[63] The present calculated reaction enthalpies indicate that: (1) the favorability of 8−5 and 8−8 linkages is higher for *p*-coumaryl than for coniferyl and sinapyl units (Figure 5); (2) cross-coupling of coniferyl and sinapyl radicals with *p*-coumaryl is favored over G−G, G−S, or S−S coupling; (3) C−C couplings involving G are relatively more favorable in cross-couplings than in self-couplings (Figures S2−S4 of Supporting Information). These results suggest that the overall regioselectivity of coniferyl radical reactions may change in the presence of *p*-coumaryl radicals, with coniferyl tending to form relatively more C−C bonds and relatively fewer C−O bonds between units. This observation can be correlated with high and low percentage of C−C and C−O linkages, respectively, in lignin of C3H and HCT down-regulated lines of alfalfa with increased *p*-coumaryl content as compared to the wild-type species.[63]

8-O-4 is generally the most favorable linkage type both in coupling and cross-coupling reactions (Figure 8). However, the

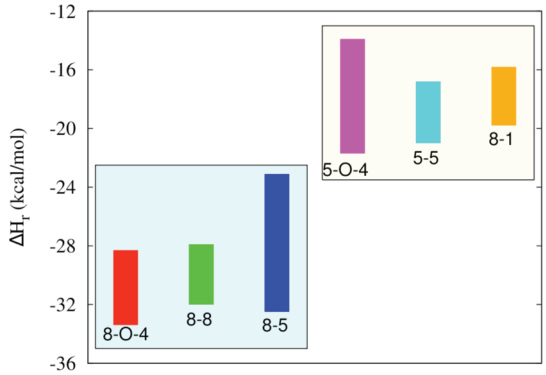

Figure 8. Range of computed ΔH_r values including self- and cross-coupling reactions for various linkages.

enthalpy of formation for this linkage is lower by only ∼2−3 kcal/mol than for the next most favorable linkages, 8-8 and 8-5. In contrast, a significant difference of 5−20 kcal/mol is found between these linkages and 5-O-4, 5-5, and 8-1 linkages. However, in natural processes and in vivo, there are other physicochemical factors that are likely to affect the linkage distribution in lignin structure. These factors include the oxidation rate of the monolignols, the orientation of the radicals during coupling and the sites available for elongation on the growing lignin polymers. The cellular environment adds further complexity to the process of lignin formation in plant cell walls. Notwithstanding, the present sets of calculations provide insight into intrinsic reactivities and set a baseline to which the above environmental effects can be referred.

■ ASSOCIATED CONTENT

Ⓢ Supporting Information

Reaction enthalpies and free energies for all self- and cross-coupling reactions, descriptions of dimeric intermediate

dx.doi.org/10.1021/jp2122449 | J. Phys. Chem. B 2012, 116, 4760−4768

geometries, and solvent effects on radical coupling reaction enthalpies. This material is available free of charge via the Internet at http://pubs.acs.org.

AUTHOR INFORMATION

Corresponding Author

*E-mail: smithjc@ornl.gov. Phone: 865-574-9635. Fax: 865-576-7651.

Notes

The authors declare no competing financial interest.

ACKNOWLEDGMENTS

This research was supported by the Bioenergy Science Center, which is a U.S. Department of Energy Bioenergy Research Center supported by the Office of Biological and Environmental Research in the Department of Energy Office of Science. This work was also supported by the National Science Foundation through TeraGrid/XSEDE computing resources provided by NCSA under Grant No. TG-MCB100173 and by the National Energy Research Scientific Computing Center (NERSC) under Grant No. m1305.

REFERENCES

(1) Bonawitz, N. D.; Chapple, C. *Ann. Rev. Genet.* **2010**, *44*, 337−363.
(2) Freudenberg, K.; Neish, A. C. *Constitution and biosynthesis of lignin*: Springer-Verlag: Berlin, 1968.
(3) Sarkanen, K, V.; Ludwig, C. H. *Lignins: occurrence, formation, structure and reactions*; Wiley-Interscience: New York, 1971.
(4) Alder, E. *Wood Sci. Technol.* **1977**, *11*, 169−218.
(5) Whetten, R.; Sederoff, R. *Plant Cell* **1995**, *7*, 1001.
(6) Chen, F.; Dixon, R. A. *Nat. Biotechnol.* **2007**, *25*, 759−761.
(7) Himmel, M. E.; Ding, S. Y.; Johnson, D. K.; Adney, W. S.; Nimlos, M. R.; Brady, J. W.; Foust, T. D. *Science* **2007**, *315*, 804.
(8) Parthasarathi, R.; Romero, R. A.; Redondo, A.; Gnanakaran, G. *J. Phys. Chem. Lett.* **2011**, *2*, 2660−2666.
(9) Kim, S.; Chmely, S. C.; Nimlos, M. R.; Bomble, Y. J.; Foust, T. D.; Paton, R. S.; Beckham, G. T. J. *Phys. Chem. Lett.* **2011**, *2*, 2846−2852.
(10) Beckham, G. T.; Matthews, J. F.; Peters, B.; Bomble, Y. J.; Himmel, M. E.; Crowley, M. F. *J. Phys. Chem. B* **2011**, *115*, 4118−4127.
(11) Ralph, J.; Lundquist, K.; Brunow, G. *Phytochem. Rev.* **2004**, *3*, 29−60.
(12) Balakshin, M.; Capanema, E.; Chang, H. M.; Jameel, H. *Planta* **2011**, *233*, 1097−1110.
(13) Miao, Y.; Liu, C. *Proc. Natl. Acad. Sci. U.S.A.* **2010**, *107*, 22728−22733.
(14) Liu, C.; Miao, Y.; Zhang, K. *Molecules* **2011**, *16*, 710−727.
(15) Aoyama, W.; Sasaki, S.; Matsumura, S.; Mitsunaga, T.; Hirai, H.; Tsutsumi, Y.; Nishida, T. *J. Wood Sci.* **2002**, *48*, 497−504.
(16) Kobayashi, T.; Taguchi, H.; Shigematsu, M.; Tanahashi, M. *J. Wood Sci.* **2005**, *51*, 607−614.
(17) Freudenberg, K. *Nature* **1959**, *183*, 1152−1155.
(18) Hatfiled, R.; Vermerris, W. *Plant Physiol.* **2001**, *126*, 1351−1357.
(19) Boerjan, W.; Raplh, J.; Baucher, M. *Annu. Rev. Plant Biol.* **2003**, *54*, 519−546.
(20) Bunzel, M.; Ralph, J. *J. Agric. Food Chem.* **2006**, *54*, 8352−8361.
(21) Rodrigues, J.; Meirer, D.; Faix, O.; Pereira, H. *J. Anal. Appl. Pyrol.* **1999**, *48*, 121−126.
(22) Beste, A.; Buchanan, A. C., III; Britt, P. F.; Hathorn, B. C.; Harrison, R. J. *J. Phys. Chem. A* **2007**, *111*, 12118−12126.
(23) Beste, A.; Buchanan, A. C., III; Harrison, R. J. *J. Phys. Chem. A* **2008**, *112*, 4982−4988.
(24) Beste, A.; Buchanan, A. C., III *J. Org. Chem.* **2009**, *74*, 2837−2841.
(25) Beste, A.; Buchanan, A. C., III *Energy Fuels* **2010**, *24*, 2857−2867.
(26) Elder, T. *Holzforschung* **2010**, *64*, 435−440.
(27) Elder, T.; Ede, R. M. *Proceedings of 8th International Symposium on Wood and Pulping Chemistry* **1995**, *1*, 115−122.
(28) Durbeej, B.; Eriksson, L. A. *Holzforschung* **2003**, *57*, 466−478.
(29) Durbeej, B.; Eriksson, L. A. *Holzforschung* **2003**, *57*, 150−164.
(30) Durbeej, B.; Eriksson, L. A. *Holzforschung* **2003**, *57*, 59−61.
(31) Besombes, S.; Robert, D.; Utille, J.-P.; Taravel, F. R.; Mazeau, K. *J. Agric. Food Chem.* **2003**, *51*, 34−42.
(32) Besombes, S.; Robert, D.; Utille, J.-P.; Taravel, F. R.; Mazeau, K. *Holzforschung* **2003**, *57*, 266−274.
(33) Besombes, S.; Mazeau, K. *Biopolymers* **2004**, *73* (3), 301−315.
(34) Besombes, S.; Utille, J. P.; Mazeau, K.; Robert, D.; Taravel, F. R. *Magn. Reson. Chem.* **2004**, *42* (3), 337−347.
(35) Chen, Y.; Sarkanen, S. *Phytochem.* **2010**, *71*, 453−462.
(36) Watts, H. D.; Mohamed, M. N. A.; Kubicki, J. D. *Phys. Chem. Chem. Phys.* **2011**, *13*, 20974−20985.
(37) Russell, W. R.; Forrester, A. R.; Chesson, A.; Burkitt, M. J. *Arch. Biochem. Biophys.* **1996**, *332*, 357−366.
(38) Allinger, N. L.; Yuh, Y. H.; Lii, J.-H. *J. Am. Chem. Soc.* **1989**, *111*, 8551−8566.
(39) Ponder, J. W.; Richards, F. M. *J. Comput. Chem.* **1987**, *8*, 1016−1024.
(40) Parr, R. G.; Yang, W. *Density-functional theory of atoms and molecules*; Oxford University Press, USA, 1994.
(41) Sousa, S. F.; Fernandes, P. A.; Ramos, M. J. *J. Phys. Chem. A* **2007**, *111*, 10439−10452.
(42) Valiev, M.; Bylaska, E. J.; Govind, N.; Kowalski, K.; Straatsma, T. P.; van Dam, H. J. J.; Wang, D.; Nieplocha, J.; Apra, E.; Windus, T. L.; de Jong, W. A. *Comput. Phys. Commun.* **2010**, *181*, 1477.
(43) Chai, J. D.; Head-Gordon, M. *Phys. Chem. Chem. Phys.* **2009**, *10*, 6615−6620.
(44) Frisch, M. J.; Trucks, G. W.; Schlegel, H. B.; Scuseria, G. E.; Robb, M. A.; Cheeseman, J. R.; Scalmani, G.; Barone, V.; Mennucci, B.; Petersson, G. A.; Nakatsuji, H.; Caricato, M.; Li, X.; Hratchian, H. P.; Izmaylov, A. F.; Bloino, J.; Zheng, G.; Sonnenberg, J. L.; Hada, M.; Ehara, M.; Toyota, K.; Fukuda, R.; Hasegawa, J.; Ishida, M.; Nakajima, T.; Honda, Y.; Kitao, O.; Nakai, H.; Vreven, T.; Montgomery, J. A., Jr.; Peralta, J. E.; Ogliaro, F.; Bearpark, M.; Heyd, J. J.; Brothers, E.; Kudin, K. N.; Staroverov, V. N.; Kobayashi, R.; Normand, J.; Raghavachari, K.; Rendell, A.; Burant, J. C.; Iyengar, S. S.; Tomasi, J.; Cossi, M.; Rega, N.; Millam, J. M.; Klene, M.; Knox, J. E.; Cross, J. B.; Bakken, V.; Adamo, C.; Jaramillo, J.; Gomperts, R.; Stratmann, R. E.; Yazyev, O.; Austin, A. J.; Cammi, R.; Pomelli, C.; Ochterski, J. W.; Martin, R. L.; Morokuma, K.; Zakrzewski, V. G.; Voth, G. A.; Salvador, P.; Dannenberg, J. J.; Dapprich, S.; Daniels, A. D.; Farkas, O.; Foresman, J. B.; Ortiz, J. V.; Cioslowski, J.; Fox, D. J. *Gaussian 09*, revision A.2; Gaussian, Inc.: Wallingford CT, 2009.
(45) Goerigk, L.; Grimme, S. *Phys. Chem. Chem. Phys.* **2011**, *13*, 6670−6688.
(46) Reed, A. E.; Curtiss, L. A.; Weinhold, F. *Chem. Rev.* **1988**, *88*, 899.
(47) Rodrigo, C. P.; James, W. H., III; Zwier, T. S. *J. Am. Chem. Soc.* **2011**, *133*, 2632−2641.
(48) Wei, K.; Luo, S.-W.; Fu, Y.; Liu, L.; Guo, Q.-X. *THEOCHEM* **2004**, *712*, 197−205.
(49) de Heer, M. I.; Korth, H.-G.; Mulder, P. *J. Org. Chem.* **1999**, *64*, 6969−6975.
(50) Zipse, H. *Top. Curr. Chem.* **2006**, *263*, 163−189.
(51) Menon, A. S.; Wood, G. P. F; Moran, D.; Radom, L. *J. Phys. Chem. A* **2007**, *111*, 13638−13644.
(52) Dewar, M. J. S.; Zoebisch, E. G.; Healy, E. F.; Stewart, J. J. P. *J. Am. Chem. Soc.* **1985**, *107*, 3902.
(53) Russell, W. J.; Burkitt, M. J.; Scobbie, L.; Chesson, A. *Biomacromolecules* **2006**, *7*, 268−273.
(54) Ruiz, E.; Cierera, J; Alvarez, S. *Coord. Chem. Rev.* **2005**, *249*, 2649−2660.

(55) Lundquist, K.; Miksche, G. E. *Tetrahedron Lett.* **1965**, 2131−2136.
(56) Setälä, H.; Pajunen, A.; Rummakko, P.; Sipila, J.; Brunow, G. *J. Chem. Soc., Perkin Trans. 1* **1999**, 461−464.
(57) Tomasi, J.; Persico, M. *Chem. Rev.* **1994**, *94*, 2027−2094.
(58) Shigematsu, M.; Kobayashi, T.; Taguchi, H.; Tanahashi, M. *J. Wood Sci.* **2006**, *52*, 128−133.
(59) Ralph, J.; Akiyama, T.; Kim, H.; Lu, F.; Schatz, P. F.; Marita, J. M.; Ralph, S. A.; Raddy, M. S. S.; Chen, F.; Dixon, R. A. *J. Bio. Chem.* **2006**, *281*, 8843−8853.
(60) Li, X.; Ximenes, E.; Kim, Y.; Slininger, M.; Meilan, R.; Ladisch, M.; Chapple, C. *Biotechnol. Biofuels* **2010**, *3*, 27.
(61) Weng, J. - K.; Mo, H.; Chapple, C. *Plant J.* **2010**, *64*, 898−911.
(62) Fu, C.; Mielenz, J. R.; Xiao, X.; Ge, Y.; Hamilton, C. Y.; Rodriguez, M.; Chen, F.; Foston, M.; Ragauskas, A.; Bouton. *J. Proc. Natl. Acad. Sci. U.S.A.* **2011**, *108*, 3803.
(63) Ziebell, A.; Gracom, K.; Katahira, R.; Chen, F.; Pu, Y.; Ragauskas, A.; Dixon, R. A.; Davis, M. *J. Biol. Chem.* **2010**, *285*, 38961−38968.